Fruit Flies Modulate Passive Wing Pitching to Generate In-Flight Turns

Attila J. Bergou,[1,*] Leif Ristroph,[1] John Guckenheimer,[2] Itai Cohen,[1] and Z. Jane Wang[3,†]

[1]*Department of Physics, Cornell University, Ithaca, New York 14853, USA*
[2]*Department of Mathematics, Cornell University, Ithaca, New York 14853, USA*
[3]*Theoretical and Applied Mechanics, Cornell University, Ithaca, New York 14853, USA*

(Received 4 October 2009; published 5 April 2010)

Flying insects execute aerial maneuvers through subtle manipulations of their wing motions. Here, we measure the free-flight kinematics of fruit flies and determine how they modulate their wing pitching to induce sharp turns. By analyzing the torques these insects exert to pitch their wings, we infer that the wing hinge acts as a torsional spring that passively resists the wing's tendency to flip in response to aerodynamic and inertial forces. To turn, the insects asymmetrically change the spring rest angles to generate asymmetric rowing motions of their wings. Thus, insects can generate these maneuvers using only a slight active actuation that biases their wing motion.

DOI: 10.1103/PhysRevLett.104.148101 PACS numbers: 87.19.lu, 47.85.Gj, 87.85.G−

To generate the vertical force necessary to sustain flight, small insects must beat their wings hundreds of times per second. Under this constraint, how do they manipulate these fast wing motions to induce flight maneuvers? Although recent studies have made progress addressing how wing motions generate aerodynamic forces [1–4], understanding how the wing motions themselves arise and what control variables govern them remains a challenge. Here, we analyze the torques fruit flies (*D. melanoaster*) exert to move their wings during sharp-turning flight. We use a moving light pattern to visually stimulate 10 such maneuvers from distinct flies [5] and measure their wing and body kinematics. By using a model of the aerodynamic forces on flapping wings, we extract the torques the insects exert to generate the wing motions. From these torques, we construct a mechanical model of the wing rotation joints that demonstrates how the interplay of aerodynamic, inertial and biomechanical forces generate the wing kinematics. Finally, we connect this model to the yaw dynamics of flies and describe the wing actuation mechanism that unifies these maneuvers.

To quantify the turning kinematics of fruit flies, we first use three orthogonal cameras to capture their flight at 8000 frames per second or about 35 frames for each wing beat [5]. The three-dimensional wing and body motion of the flies is then reconstructed from these videos using Hull reconstruction motion tracking (HRMT) [6]. In what follows, we analyze turns ranging between 5° and 120° and present details of the analysis for the largest of these. The body kinematics, described by the centroid coordinates and three Euler angles—yaw, ϕ_b, body pitch, θ_b, and roll, ψ_b, during a turn are shown in Fig. 1(a) and visualized in Fig. 1(b). During the level flight, the fly performs a 120° turn in 80 ms, or 18 wing beats. To induce such a turn, the insect generates differences between the motion of its left and right wings. We quantify these changes by plotting in Fig. 1(c) the time course of three Euler angles—stroke, ϕ, deviation, θ, and wing pitch, ψ—that describes the orientation of the wings relative to the hinges about which they rotate. A three-dimensional representation of a typical wing stroke is shown in Fig. 1(d).

During the maneuver, asymmetries appear in all three wing angle kinematics, however, not all of these are involved in inducing the turn. For example, the most apparent asymmetry—the shift in the mean stroke angles of the wings—simply reorients the aerodynamic forces about the yaw axis of the fly and does not affect the torque that causes the turn. To gauge the importance of the wing motion asymmetries for inducing the turn, we use a quasisteady aerodynamic model [7] to determine the average yaw torque generated by the wing beats from $t =$ 10–30 ms, when the fly begins to turn. We compare this value to the torque generated by wing motions for which two of the three wing angle kinematics are symmetrized to the left-right average, isolating the asymmetry in the third. The asymmetry between the wing pitch angles alone generates a yaw torque that is 98% of the total torque generated when all the asymmetries are present. The other 2 degrees of freedom generate less than 3% of the total torque. These results indicate that the fly manipulates its wing pitch to induce the turn.

To quantify the wing pitch asymmetry that induces the turn, we phase average [8] the strokes from $t = 10$–30 ms [Fig. 1(e)]. We find that, on the front stroke, the right wing flaps with an average midstroke angle of attack of $\alpha = 49°$ while, on the back stroke, it flaps with $\alpha = 40°$. The higher α on the front stroke indicates that a larger area of the wing is presented to the flow, resulting in a larger drag force. This force causes average yaw torques of -19.7 and 14.7 nN m, respectively, on the front and back strokes that turn the fly rightward. The left wing flaps with $\alpha =$ 48°, for the front-stroke, and $\alpha = 50°$, for the back stroke, generating average yaw torques of 21.7 and -22.5 nN m, respectively. Because of the close values of α during the

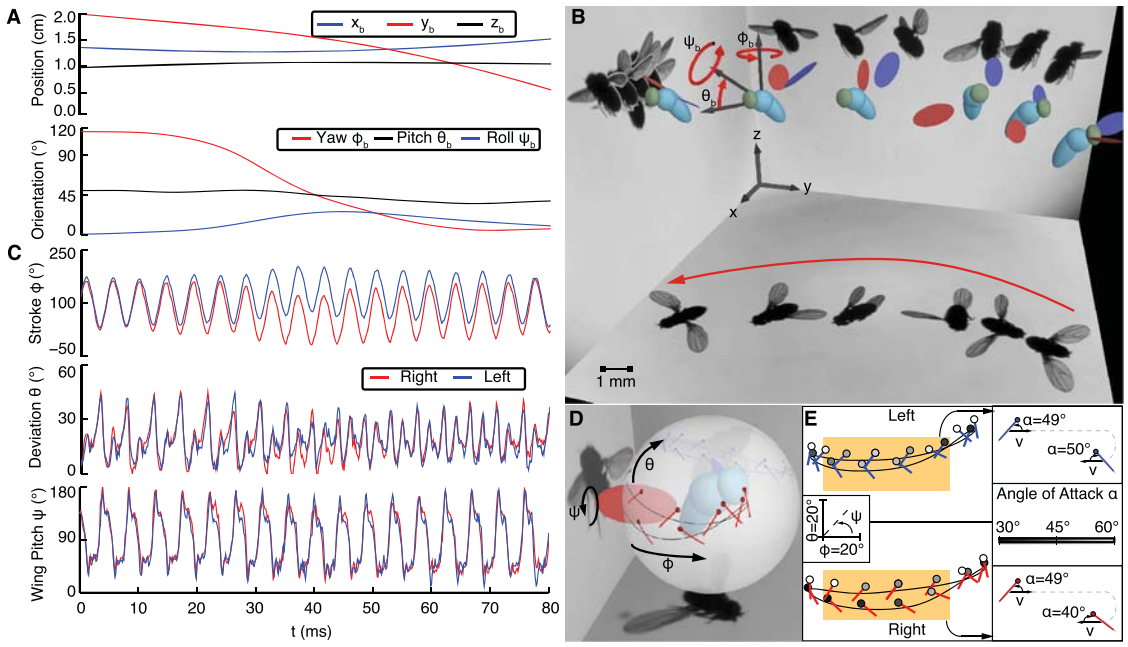

FIG. 1 (color online). (a) Fly body position and orientation vs time. Measurement uncertainties are 0.05 mm and 3°, respectively [6]. (b) Motion reconstruction of the 120° turn. The side panels show 6 of 821 frames recorded by high speed videography. Labeled on the fifth frame are the Euler angles that quantify the fly's orientation. (c) Fly wing orientation relative to body vs time. Measurements are accurate to approximately 3° [6]. The wings are chiefly driven by the same large flight muscles resulting in motion that is nearly in phase [10]. (d) Trajectory and orientation of wing chords during a typical flapping stroke. The ball and sticks on the globe depict the chord's orientation at equal time snapshots, with the ball depicting the wings leading edge. Three Euler angles describe each wing's orientation within the stroke plane (ϕ), deviation from the stroke plane (θ), and orientation around its span (ψ). (e) The unwrapped ball-and-stick diagram highlights the 9° asymmetry in the midstroke angle of attack α that induces the maneuver. The uncertainty in α is approximately 1°.

front and back strokes, the torques nearly cancel. Thus, by varying pitch, and consequently angle of attack, of its right wing the fly rows through the air to perform the turn.

To elucidate how the fly controls its wing pitch, we invert the equations of motion of the wings to determine the torque the fly exerts at the wing hinge,

$$\vec{\tau} = \mathbf{I}_w \cdot \dot{\vec{\omega}} - \vec{r} \times m_w \vec{a} - \vec{\tau}_a. \quad (1)$$

From kinematic data, we determine the rotational acceleration $\dot{\vec{\omega}}$ and acceleration $\vec{a}$ of the wing centroid. We also measure the wing mass $m_w = 2.7 \pm 0.3$ μg, span $s = 2.02 \pm 0.05$ mm, and chord $c = 1.02 \pm 0.05$ mm. The wing moment of inertia I_w and center of mass-to-hinge vector $\vec{r}$ are estimated from an elliptical disc wing rotating about a point at its leading edge one quarter chord below its base [9]. The total torque that aerodynamic forces exert about the wing hinge, $\vec{\tau}_a$, is calculated using a quasisteady model [7]. From Eq. (1), we determine the torque component flies exert to pitch their wings, τ_p, during the turn and during steady flight.

Previous studies have suggested that the pitching torques result from torsional deformation of the wing hinge and wing itself and simply resist the tendency of inertial [9–11] and aerodynamic [12–15] forces to flip the wing. To integrate these ideas into a dynamical model for the pitching torque, we plot τ_p versus ψ in Fig. 2(a) for the final 9 consecutive strokes associated with steady flight in Fig. 1(c). The torque data trace out an elliptical curve whose major axis has a negative slope. This negative correlation indicates that when the wing angle deviates from approximately 90°, the hinge produces a restoring torque like a spring. The area enclosed by the ellipse indicates the energy dissipated by the hinge as it pitches the wing. These data suggest the hinge acts like a damped torsional spring,

$$\tau_p = -\kappa(\psi - \psi_0) - C\dot{\psi}, \quad (2)$$

where the parameters κ, C, and ψ_0 correspond, respectively, to the torsion constant, damping constant, and the rest angle of the torsional spring. We fit this model to all 9 wing strokes, finding values $\kappa = 91 \pm 9$ pN m/°, $C = 39 \pm 12$ fN m s/°, and $\psi_0 = 90 \pm 1°$ that account for 95% in the variance of the pitching torque [Fig. 2(a)].

To determine how the wing pitch is actuated differently during the turn, the above analysis is repeated for the 5 strokes that induce the turning maneuver. We find that Eq. (2) also accounts for the exerted torques during these wing beats. The phase-averaged τ_p versus ψ for the 5 asymmetric strokes and the 9 symmetric steady strokes are compared in Fig. 2(b). The two loops are shifted

horizontally with respect to each other, indicating a change in ψ_0, the wing's rest angle. In fact, by plotting the values for κ, C, and ψ_0 as a function of time, we show that only ψ_0 varies significantly throughout the maneuver [Figs. 3(a)–3(c)]. The steadiness of κ and C suggests these parameters represent material properties of the wing hinge [11]. Comparison of the parameter values with the fly's yaw dynamics in Fig. 3(d) indicates that, to induce the rightward turning maneuver, the insect increases the ψ_0 of the right wing relative to the left by about 15° for 5 strokes. This is followed by two wing beats for which ψ_0 of the right wing is decreased relative to the left by about 10°. The sign reversal of $\Delta\psi_0 = \psi_0^{(l)} - \psi_0^{(r)}$ generates a countertorque that slows the fly's yaw velocity. In the final 9 wing strokes, the ψ_0 values for the left and right wings are nearly equal so that no active torque is generated.

To validate that the fly's yaw dynamics derives from changes to the relative rest angle of the wings $\Delta\psi_0$, we simulate the coupled wing-body dynamics in a model fly. The driving of each wing is simulated by prescribing its stroke and deviation angles. The fly's wing pitch and yaw angles are then determined from the interaction of the spring model in Eq. (2) with the aerodynamic forces on the wings [5]. To form a minimal model of the turn, the variables κ and C are held constant [dashed lines in Figs. 3(a) and 3(b)], θ is set to zero, and ϕ is driven purely sinusoidally with no offset between the wings. The flapping amplitude and frequency is matched to the experiments. The wing rest angles ψ_0 are prescribed by the dashed lines in Fig. 3(c), which capture the observed gross features and ensure that locally the area between the dashed lines matches the area enclosed between the two experimental curves. In Fig. 3(d) the measured yaw dynamics are compared to the turning model prediction. The model prediction quantitatively matches experimental measurements of the time course of the turn. In Fig. 3(e), the measured wing pitch angles are compared with model predictions for the three regions that correspond to $\Delta\psi_0 < 0$, $\Delta\psi_0 > 0$, and $\Delta\psi_0 \approx 0$. We find the minimal model recovers the average measured wing pitch asymmetries, which are sufficient to drive the turn. Simulation of experimentally measured wing ϕ and θ angles without asymmetries in the rest angle, $\Delta\psi_0 = 0$, does not lead to asymmetric wing pitch angles and does not yield a rightward turn. Similarly, we find that changes to $\Delta\psi_0$ alone explain the time course of all 10 turns we analyze [5].

To show how flies modulate their wing pitch to generate different turn angles, we relate their body yaw and wing pitching dynamics [Fig. 4(a)]. Flies induce a turn by adjusting the rest angles of their wings to break the symmetry of their strokes. The change in ψ_0 alters the resistive torque exerted by the wing hinge, affecting the wing pitch and giving rise to distinct angles of attack on the front stroke and back stroke. This asymmetry in α generates a net thrust during a wing beat and a yaw torque on the flies. Thus, by shifting their left-right wing rest angles we find that flies induce a linear shift between their wing pitch angles so that $\Delta\psi \approx \mu\Delta\psi_0$ [Fig. 4(b)]. The asymmetric

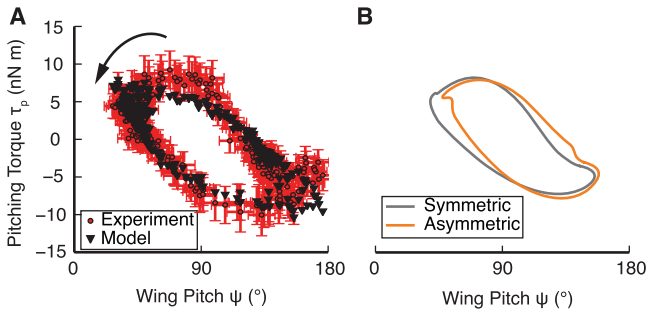

FIG. 2 (color online). (a) Pitching torque vs wing pitch for the wing beats during steady flight. Circles are instantaneous values corresponding to frames of the flight sequence. Triangles are the result of fitting τ_p with a damped torsional spring model. The counterclockwise direction of propagation indicates that the motion is damped. (b) Phase-averaged τ_p vs ψ for strokes associated with symmetric wing movements compared to asymmetric wing movements.

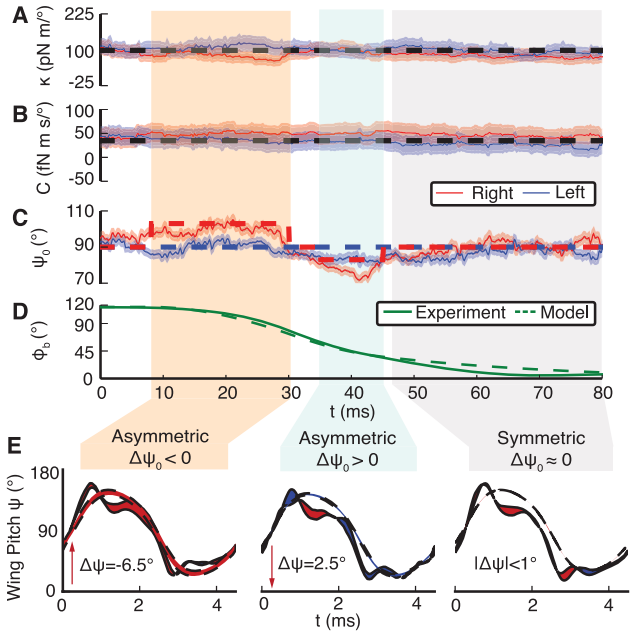

FIG. 3 (color online). (a)–(c) Torsional spring parameters vs time extracted with error bars from experimental data. Dashed lines are the parameter values simulated in the minimal turning model. (d) Yaw angle vs time. Measurements (solid line) are compared with turning model simulations (dashed line). (e) Phase-averaged wing pitch vs time in the three labeled regions for measurements (solid lines) and the turning model (dashed lines). The area between the left and right wing curves is shaded to correspond to the wing whose pitch is shifted up. The mean shift $\Delta\psi$ in the three regions are 6.5° (asymmetric $\Delta\psi_0 < 0$), 2.5° (asymmetric $\Delta\psi_0 > 0$), and <1.0° (symmetric $\Delta\psi_0 \approx 0$). The corresponding $\Delta\psi$ for the turning model are 8°, 2.9°, and 0°, respectively.

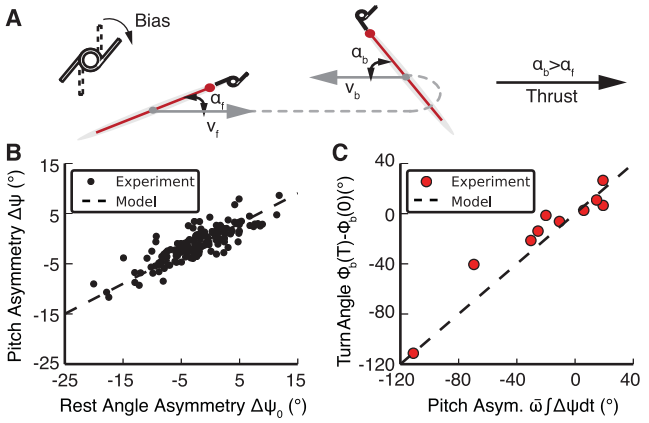

FIG. 4 (color online). (a) Minimal model of turning dynamics. Biasing the spring rest angle produces an asymmetric stroke that generates thrust and a yaw torque on the fly. (b) The average values of $\Delta\psi$ vs $\Delta\psi_0$ for 147 strokes (circles) compared with simulations of the turning model (dashed line). Measurement errors are on the order of the data spread and omitted for clarity. (c) Turn angle vs cumulative pitch asymmetry. Measurements (circles) are compared with predictions of the turning model (dashed line). Measurement errors are on the order of the marker size and omitted for clarity.

wing motions generate an active yaw torque that is linearly proportional to $\Delta\psi$ [5] and a passive countertorque [16–19]. The flies' yaw motion is described by

$$I_b\ddot{\phi}_b + 2\bar{\omega}C_\tau\dot{\phi}_b = 2C_\tau\bar{\omega}^2\Delta\psi \approx 2C_\tau\bar{\omega}^2\mu\Delta\psi_0, \quad (3)$$

where I_b is the moment of inertia of the fly about the yaw axis, C_τ is a parameter that depends on the wing drag coefficient and geometry, $\bar{\omega}$ is the average angular velocity of the wings, and ϕ_b is the yaw of the body [5]. Experimental analysis of 147 distinct wing strokes yields $\mu = 0.51 \pm 0.03$, which compares well with simulations of the minimal flapping model that gives $\mu = 0.6$. Integrating Eq. (3) over time gives the total turn angle of a fly starting and ending at rest,

$$\phi_b(T) - \phi_b(0) = \bar{\omega}\int\Delta\psi dt \approx \bar{\omega}\mu\int\Delta\psi_0 dt. \quad (4)$$

We confirm that Eq. (3) accounts for the observed yaw dynamics of flies by plotting $\phi_b(T) - \phi_b(0)$ versus $\bar{\omega}\int\Delta\psi dt$ for 10 turning maneuvers in Fig. 4(c). The yaw angles of the measured turns are in excellent agreement with the prediction of Eq. (4). Thus, by changing the strength and duration of the asymmetry in wing rest angles, flies can control their turn angle.

Taken together, our findings reconcile how flies combine active and passive modulation of their wing kinematics to control their flight [9–11,15,19,20]. In all forms of locomotion—aquatic, terrestrial, and aerial—animals take advantage of mechanical properties of their bodies to simplify the complex actuation necessary to move [21]. We find that, for fruit flies, the mechanical properties of the wing hinge appear to be finely tuned to enable modulation of their wing pitch through only slight active actuation. The springlike behavior of the wing hinge also connects the time scale of a turning maneuver with the time scale of the wing actuation. Our model predicts that flight muscles of flies can act over several wing beats to bias the pitch of the wings and yet generate the sub-wing-beat changes in wing motion that aerodynamically induce the maneuver. Finally, because animals over a wide range of length scales experience similar rotational dynamics [16], the simple mechanism used by fruit flies may be quite general and should likewise simplify the control of flapping flying machines.

We thank A. Ruina, G. Berman, K. Jensen, S. Chang for helpful discussions. This work is supported by NSF.

*ajb78@cornell.edu
†zw24@cornell.edu

[1] S. Fry, R. Sayaman, and M. H. Dickinson, Science **300**, 495 (2003).
[2] C. P. Ellington, Phil. Trans. R. Soc. B **305**, 1 (1984).
[3] S. P. Sane, J. Exp. Biol. **206**, 4191 (2003).
[4] Z. J. Wang, Annu. Rev. Fluid Mech. **37**, 183 (2005).
[5] See supplementary material at http://link.aps.org/supplemental/10.1103/PhysRevLett.104.148101 for technical details related to this Letter.
[6] L. Ristroph, G. J. Berman, A. J. Bergou, Z. J. Wang, and I. Cohen, J. Exp. Biol. **212**, 1324 (2009).
[7] U. Pesavento and Z. J. Wang, Phys. Rev. Lett. **93**, 144501 (2004).
[8] S. Revzen and J. M. Guckenheimer, Phys. Rev. E **78**, 051907 (2008).
[9] A. R. Ennos, J. Exp. Biol. **140**, 161 (1988).
[10] J. A. Miyan and A. W. Ewing, J. Exp. Biol. **136**, 229 (1988).
[11] A. R. Ennos, J. Exp. Biol. **140**, 137 (1988).
[12] A. M. Mountcastle and T. L. Daniel, Exp. Fluids **46**, 873 (2009).
[13] J. Toomey and J. D. Eldredge, Phys. Fluids **20**, 073603 (2008).
[14] M. Vanella, T. Fitzgerald, S. Preidikman, E. Balaras, and B. Balachandran, J. Exp. Biol. **212**, 95 (2009).
[15] A. J. Bergou, S. Xu, and Z. J. Wang, J. Fluid Mech. **591**, 321 (2007).
[16] T. L. Hedrick, B. Cheng, and X. Deng, Science **324**, 252 (2009).
[17] B. Etkin and L. D. Reid, *Dynamics of Flight: Stability and Control* (Wiley, New York, 1995).
[18] T. Hesselberg and F.-O. Lehmann, J. Exp. Biol. **210**, 4319 (2007).
[19] L. Ristroph, A. J. Bergou, G. Ristroph, K. Coumes, G. Berman, J. Guckenheimer, Z. J. Wang, and I. Cohen, Proc. Natl. Acad. Sci. U.S.A. **107**, 4820 (2010).
[20] M. H. Dickinson, F.-O. Lehmann, and K. G. Götz, J. Exp. Biol. **182**, 173 (1993).
[21] M. H. Dickinson, C. T. Farley, R. J. Full, M. A. R. Koehl, R. Kram, and S. Lehman, Science **288**, 100 (2000).